

H. Terato and T. Saito¹

Analytical Research Center for Experimental Sciences,
Saga University

¹Research Reactor Institute, Kyoto University

INTRODUCTION: Ionizing radiation causes densely accumulated damage cluster in the target DNA molecule. Among various ionizing radiations, heavy ion particle can produce more expanding ionization domain around their track than low-LET ionizing radiation such as gamma-ray. Therefore heavy ion particle cause more densely accumulated damage cluster in the target DNA, termed clustered DNA damage (CDD). The complex structure of CDD is thought to lead its less-repairability and inhibition of DNA replication. Thus CDD seems to be a major factor responsible to severity of radiobiological consequence [1]. On the other hand, a lot of previous studies have presented no certain correlation between yields of CDD and radiation effect. Since we considered that it is based on the condition-sensitive character of CDD, we here estimated yields of CDD in various conditioned irradiation experiments with heavy ion particle and gamma rays. Yields of intracellular CDD decreased as LET of the radiations grew. Also the yields of CDD were modified by some irradiation conditions such as oxidation status and ionic strength.

EXPERIMENTS: Exponentially growing chinese hamster ovary (CHO) AA8 cells were irradiated by gamma-ray (0.2 keV/ μ m), and carbon (13 keV/ μ m), silicon (55 keV/ μ m) and argon (90 keV/ μ m) particle beams, respectively (parenthetic numbers indicate respective LETs). The irradiated cells embedded in agarose plugs were analyzed with static field agarose gel electrophoresis. For estimation of CDD containing oxidative base lesions (BLC), the plugs were treated by endonuclease III and Fpg before electrophoresis. The detail of analysis procedure was based on our previous report [2]. For condition-sensitive character of radiation effect, we estimated CDD in purified pUC19 plasmid DNA irradiated by carbon, silicon and iron (200 keV/ μ m) ion particles in various aqueous solutions mentioned below.

RESULTS: The total yields of intracellular CDD as sum of double strand break (DSB) and BLC decreased as LET of the radiations grew (Fig. 1). The major decrement fractions were BLCs but not DSBs. It suggests the different generation mechanism of DSB and base lesions. The result corresponds with our previous in vitro data [2].

A lot of previous studies have not presented a certain correlation between yields of CDD and radiation effect. Especially, radiation effect in aqueous system such as

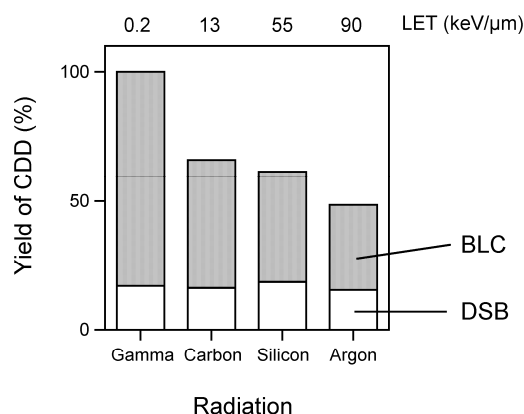


Fig. 1. Yields of intracellular CDD in irradiated cells.

biological system is easily affected by irradiation conditions such as scavenging ability for reactive oxygen species of the solvent. Considering condition-sensitive character of radiation effect, we estimated CDD in purified pUC19 plasmid DNA irradiated by various ion particles in various aqueous solutions. 10 μ M hydrogen peroxide and Fenton reagent increased 15.6% and 32.2% of the CDD induced by carbon particle beams, respectively. Additional oxidative state showed similar additive damaging effect for silicon irradiation, but not iron irradiation. Since we usually use relatively high concentrated salt for mimic of intracellular radical scavenging condition, we evaluated species of salts in the solution for yields of CDD. Yields of CDD in 0.4 M sodium phosphate buffer (pH 7.5) were 9.7% and 16.4% lower than those in 10 mM phosphate buffer at 25 Gy carbon and silicon irradiations, respectively. On the other hand, there was no such damage-reduction effect in 0.4 M potassium phosphate buffer. These results are partially conformed to our previous report showing radio-protection ability of 2 M sodium chloride for gamma-irradiated DNA [3].

Conclusively, the yields of CDD induced by heavy particle beams showed inversely proportional to their LETs. It suggests that yields of CDD are not simply responsible to severity of radiobiological consequence. The yields showed susceptible to irradiation condition, leading to change of expression of radiation effect. It also bedims the impact of CDD on radiation effect for us. We need further experiments with cautious approach to irradiation conditions.

REFERENCES:

- [1] H. Terato and H. Ide, *Biol. Sci. Space*, **18** (2004) 206-215.
- [2] H. Terato *et al.*, *J. Radiat. Res.*, **49** (2008) 133-146.
- [3] M. M. Ali *et al.*, *J. Radiat. Res.*, **45** (2004) 229-237.

T. Tachizawa¹, M. Takagaki¹, K. Ohyama², T. Tomaru³,
S. Masunaga⁴, N. Kondoh⁴ and K. Ono⁴

Dept of Neurosurgery, Kanto Rosai Hospital

¹Faculty of Nursing, Aino Gakuin College

²Dept of Neurosurgery, Kameoka Shimizu Hospital

³Sakura Medical Center, Toho University

⁴Research Reactor Institute, Kyoto University

Question: Whether does TMZ disturb up-taking of BPA into tumor cell, or not?

An Anti-tumor agent, Temozolomide (TMZ), has been widely recognized as the 1st choice for glioma chemotherapy [1]. TMZ causes serious DNA damage by methylating the O6-position of guanine. The main mechanisms of tumoricidal effect of TMZ are not by apoptosis, but by G2 arrest of tumor cell [2]. Furthermore, autophagy was observed in the damaged tumor cell treated by TMZ, in which self-organelles of the damaged tumor cell were digested via phagocytosis [3]. Thus, TMZ may decrease BPA up-take into seriously damaged tumor cell via its metabolic process and may be incompatible with BPA-based BNCT.

Case: 76y old female made complaints progressive right hemiparesis and aphasia, and was diagnosed via open biopsy as anaplastic astrocytoma, grade-III glioma, of left motor area as shown in Fig.1. Immediately after the diagnosis, TMZ 100mg / day was administrated intravenously for 3 weeks before BNCT. However, FBPA-PET unusually revealed small up-take of BPA, the T/N ratio = 1.66, then BNCT became out of scope for its low T/N ratio since >3.0 is prerequisite for the T/N ratio of BPA-based BNCT. Fortunately, the tumor shrunken in more than 30%, then conventional radiation therapy and chemotherapy have been applied.



Fig.1. left:MRI_Gd-T1, middle:CT, right:FBPA-PET.

Experiments: In this study, an effect of TMZ onto the up-taking of BPA into tumor cells has been investigated. A172 glioma cells were treated with BPA-based BNCT with/without pretreatment of various concentration of TMZ. In our *in-vitro* experimental conditions, TMZ did not show any synergetic/anti-synergetic effect with BPA-based BNCT effect as shown in Fig. 2. TMZ only showed high toxicity in a dose dependent manner.

Conclusion: Pre-treatment of TMZ in *in-vitro* conditions might not deny BPA-based BNCT.

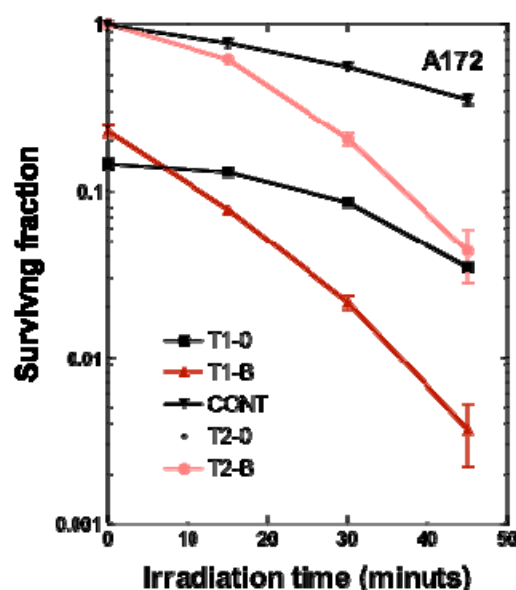


Fig.2. Survival fraction post BNCT on A172 glioma cell pretreated with BPA and TMZ. (▼:control, ■:BPA, ■:TMZ+ ▲:TMZ+BPA)

- [1] E. Yaman, S. Buyukberber, M. Benekli, Y. Oner, U. Coskun, M. Akmansu, B. Ozturk, AO. Kaya, D. Uncu, R. Yildiz *Clin Neurol Neurosurg* **112**(8) (2010) 662-667.
- [2] Hirose Y, Berger MS, Pieper RO *Cancer Res* **61** (2001) 47-63.
- [3] Kanazawa T, Bedwell J, Kondo Y *et al. J Neurosurg* **99** (2003)1047-1052.

C.M. Lee^{1,2}, M. Sasai², M. Suzuki³ and Y. Sakurai³

Graduate School of Medicine, Osaka University

¹*Department of Health Economics and Industrial Policy*

²*Medical Center for Translational Research*

³*Research Reactor Institute, Kyoto University*

INTRODUCTION: Pleural mesothelioma is a lethal disease caused by exposure to asbestos. The current therapy for pleural mesothelioma is multidisciplinary; surgery, chemotherapy, and radiotherapy. However, surgery (extrapleural pneumonectomy) is limited to locally advanced pleural mesothelioma. Chemotherapeutic regimens with CDDP and Pemetrexed have resulted in an improved tumor response, but the median survival is still only 12 months from the date of diagnosis. The use of radiotherapy, including intensity-modulated radiotherapy (IMRT), is limited because the extent of the tumor requires large fields and it is impossible to administer tumoricidal doses without injuring the adjacent lung and mediastinal organs [1, 2]. BNCT could be a breakthrough strategy to treat pleural mesothelioma, because it is suitable for the treatment of diffuse and invasive tumor [3, 4]. However, the success of BNCT depends on the selective delivery of ¹⁰B-atoms to tumor cells to complement the attenuation of thermal neutron. BNCT is done against the tumors that occupied near the body surface area efficiently. Concerning BNCT for pleural mesothelioma, novel compound that possesses high affinity to tumor cells than conventional boron compounds are craved for BNCT for pleural mesothelioma.

We developed novel boron compound that bound with pleural mesothelioma cells preferentially, and examined the efficiency of BNCT for pleural mesothelioma bearing mice.

EXPERIMENTS: Boron compound were prepared by Professor Nakamura (Gakusyuin University). Pleural mesothelioma bearing mice were prepared by murine pleural mesothelioma cell injection into the pleural cavity on day0. On day 6, mice were transported from Osaka University to KUR, and 10,000 ppm or 2,00 ppm of each

boron compound was administrated on day7. On day8, Neutron irradiation to pleural mesothelioma bearing mice was performed 2 h after 10,000 ppm of BSH administration. The mice were then set the acryl stand, and irradiated at KUR. In the in-air beam characteristics, thermal neutron flux and the γ -ray absorbed dose were 1.1×10^{12} neutrons/cm² and 0.4 Gy at a reactor power of 1 MW for 40 minutes, respectively.

RESULTS: Unfortunately, the mice were dead due to unknown reason after the administration of each boron compound. We performed the same experiments under the same protocol at JRR-4. The mice that used at JRR-4 were dead by the progress of bearing tumor after neutron irradiation without accidental reason. So the statistical analyses were not performed in the experiments of KUR. We will clean up the reason in the near future.

REFERENCES:

- [1] D.C. Rice *et al.*, *Int J Radiat Oncol Biol Phys*, **69** (2007)350-357.
- [2] A.M. Allen *et al.*, *Int J Radiat Oncol Biol Phys*, **65** (2006) 640-645.
- [3] M. Suzuki *et al.*, *Jpn J Clin Oncol.*, **37** (2007) 245-249.
- [4] M. Suzuki *et al.*, *Radioth Oncol.* **88** (2008) 192-195.

T. Fujimoto, T. Andoh¹, Y. Sakurai², S. Kawabata³, M. Suzuki², H. Ichikawa¹ and K. Ono²

Hyogo Cancer Center,

Department of Orthopaedic Surgery

¹Faculty of Pharmaceutical Sciences and Cooperative

Research Center of Life Sciences,

Kobe Gakuin University

²Research Reactor Institute, Kyoto University

³Osaka Medical College,

Department of Neurosurgery

INTRODUCTION: Clear cell sarcoma (CCS), a rare malignant tumor with a predilection for young adults [1], demonstrates poor prognosis [2]. Recently, however, boron neutron capture therapy (BNCT) with the use of *p*-boronophenylalanine (BPA) for malignant melanoma has provided good results [3]. Since BPA is used for the production of melanin, boron finally accumulates in tumor cells. Also, since CCS produces melanin, the uptake of BPA is the key to using BNCT for CCS. Here, we evaluated the uptake of BPA with the use of CCS cell lines and produced a tumor-bearing animal model of CCS with the use of nude mice. The melanin produced by the tumor was histologically examined and the accumulation of boron was quantitated in the tumor-bearing animal model produced for BNCT.

EXPERIMENTS:

(1) *Boron concentration in CCS:* Human cell lines, MP-CCS-SY [4], SU-CCS-1 [5], Kas [6] and HS-MM [7] were grown in RPMI 1640 and DMEM (for HS-MM) with fetal bovine serum in a 5% CO₂ humidified incubator at 37°C. Each CCS cell line was cultured in a culture dish for 72 h and exposed to BPA (Stera Pharma Co., Osaka, Japan) in the medium for 4 h. The cells were washed, detached and collected; boron concentration was then measured by ICP-AES.

(2) *Tumor-bearing animal model of CCS:* Cells of each CCS cell line were subcutaneously transplanted into each BALB/c nude mouse. Four weeks thereafter, the animal was killed and the tumor mass was resected. Histological examination was carried out by HE staining, immunohistochemical examination by melan A, HMB-45 and S-100 protein, and the molecular genetic technique for the detection of the chimeric EWS/ATF1 [8] gene by RT-PCR for confirming CCS.

(3) *Boron concentration in CCS-bearing animal model:* BPA (500mg/kg) was intravenously administered through the femoral vein to the tumor-bearing (MP-CCS-SY) anesthetized nude mice. Thereafter, at predetermined time intervals, the mice were killed, their tissue samples

collected immediately, and the boron in the samples was quantitated by the ICP-AES method.

(4) *BNCT for CCS(MP-CCS-SY)-bearing animal model:* BNCT was carried out on the BPA-administered, CCS-bearing nude mice.

RESULTS: With the use of BPA, a high accumulation of boron was, for the first time, shown in CCS. The four cell lines incorporated the boron in a concentration-dependent manner. In the tumor-bearing animal model, each of the four cell lines produced the same solid tumor mass. Microscopically, CCS was composed of nests of monotonous polygonal cells with clear cytoplasm but displayed no melanin pigment upon HE staining. As evaluated by immunohistochemistry, each cell line was positive. Moreover, the presence of the EWS/ATF1 fusion gene confirmed that the tumor-bearing animal model was prone to the recurrence of CCS. Since the culture study showed the potentiality of BNCT for CCS, further clinical investigation into the use of BNCT could be pursued with the use of this animal model. Bio-distribution of boron after the intravenous administration of BPA revealed tumor-specific and high-level boron accumulation in the tumor mass [Fig. 1]. The highest concentrations of boron in the tumor was 45 ppm. The tumor-to-blood (T/B) and tumor-to-skin (T/S) ratio was 7.5 and 7.8, respectively. The effect of BNCT on the CCS-bearing animal model is currently under analysis.

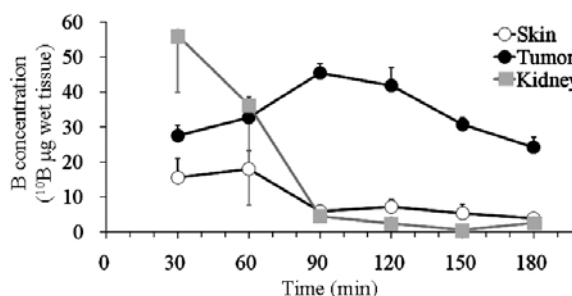


Fig. 1. Time course changes of boron concentration in tumor, skin and kidney after intravenous administration of BPA (500 mg/kg).

REFERENCES:

- [1] F.M. Enzinger, *Cancer*, **18**(1965) 1163-1174.
- [2] W. Deenik et al., *Cancer*, **86**(1999) 969-975.
- [3] Y. Mishima et al., *Lancet*, **12**(1989) 388-389.
- [4] H. Moritake et al., *Cancer Genet. Cytogenet.*, **135**(2002) 48-56.
- [5] A. L. Epstein et al., *Cancer Res.*, **44**(1984) 1265-1274.
- [6] M. Jishage et al., *Oncogene*, **22**(2003) 41-49.
- [7] H. Sonobe et al., *J. Pathology*, **169**(1993) 317-322.
- [8] J. Zucman et al., *Nat. Genet.*, **4**(1993) 341-345.

M. Yanaga, H. Shimoyama¹, H. Tanaka¹, and Y. Nakano²

*Radiochemistry Research Laboratory,
Faculty of Science, Shizuoka University*

¹*Department of Chemistry, Graduate School of Science,
Shizuoka University*

²*Research Reactor Institute, Kyoto University*

INTRODUCTION: Zinc (Zn) is one of the most important elements in living organisms because of its various functions in metalloenzymes including catalytic, structural, and regulatory roles. Zn deficiency leads to various symptoms, such as skin injury, alopecia, loss of senses, impaired wound healing, growth retardation.

Zn interacts with many other trace metal elements. Previously, we determined trace elements in liver, pancreas, testis, bone and other tissues of mice [1–4]. Cobalt concentration increased significantly in all the organs and tissues of Zn-deficient mice, whereas Zn concentration in liver and kidney was not distinctly decreased. However, Zn concentrations in pancreas and bone in Zn-deficient mice were significantly decreased. In the present work, the concentrations of trace elements in subcellular fractions of pancreata and testes of Zn-deficient mice were determined in order to investigate the behavior and role of Zn and other trace elements.

EXPERIMENTS: *Animals and samples* Male mice of the ICR/jcl strain, 8-week-old, were divided into two groups. One group was fed with Zn-deficient diet and ultra pure water (Zn-def. mice) and the other with control diet and the same water (control mice) for a week. After treatment period, their pancreata, testes, and other organs and tissues were removed under diethyl ether anesthesia. The removed pancreata and testes of every four mice of each group were together homogenized with HEPES buffer because each pancreas or testis is too small for analysis. The homogenates were separated into fractions, such as nuclear, mitochondrial, microsome and cytosolic fractions, by differential centrifugation at 1,000×g for 20 min, 9,000 ×g for 20 min and 105,000×g for 65 min, respectively. They were weighed, freeze-dried, weighed again and grounded. Each sample (10 - 50 mg) was doubly wrapped in a polyethylene film and subjected to INAA (Instrumental Neutron Activation Analysis).

INAA The samples in polyethylene capsules were

irradiated in Pn-1 for 6 minute and for 2 hours, for short and long irradiation, respectively. As comparative standards, the certified NIST Standard Reference Material 1577b Bovine Liver as well as elemental standard for Mg was used. The γ -ray spectroscopic measurements with an HPGe detector were performed repeatedly for the short-irradiated samples: the first measurements for 120 – 600 seconds after decay time of 5 - 10 minutes and the second one for 250 - 1800 seconds after 60 - 150 minutes. The long-irradiated samples were measured for 10 - 72 hours after an adequate cooling time (15 - 60 days).

RESULTS: Concentrations of ten elements, Na, Mg, Cl, Mn, Fe, Co, Cu, Zn, Se and Rb, were determined. The Zn concentrations in mitochondrial and cytosolic fractions of pancreatic cells of Zn-deficient mice were distinctly lower than those of control mice. On the other hand, the Co concentrations in all subcellular fractions, especially in nuclear and cytosolic fractions, of Zn-deficient mice were increased.

SDS-PAGE and 2D electrophoresis were carried out for cytosolic fractions of pancreata and testes of other mice. Proteins in the cytosolic fraction were also separated into twenty fractions by gel-filtration chromatography. After that, SDS-PAGE was performed for each fraction. New bands were found on the gel for a few fractions of pancreatic cells of Zn-deficient mice.

REFERENCES:

- [1] M. Yanaga, M. Iwama, K. Takiguchi, M. Noguchi and T. Omori, *J. Radioanal. Nucl. Chem.*, **231** (1998) 187-189.
- [2] M. Yanaga, M. Iwama, K. Shinotsuka, K. Takiguchi, M. Noguchi and T. Omori, *J. Radioanal. Nucl. Chem.*, **243** (2000) 661-667.
- [3] M. Yanaga, H. Wakasa, T. Yoshida, M. Iwama, K. Shinotsuka, M. Noguchi and T. Omori, *J. Radioanal. Nucl. Chem.*, **245** (2000) 255-259.
- [4] T. Ogi, Y. Kawamoto, H. Maetsu, M. Koike, T. Ohyama, S. Enomoto, M. Noguchi, H. Suganuma and M. Yanaga, *Proc. Intern. Symp. on Bio-Trace Elements 2002* (2000) 83.

M. Okumura^{1,4}, Y. Hidaka², K. Tao¹, G. Inoue¹, T. Maekawa¹, L. Ito¹, N. Fujii³, N. Fujii³ and H. Yamaguchi¹

¹*School of Science and Technology, Kwansai Gakuin University*

²*Graduate School of Science and Engineering, Kinki University*

³*Research Reactor Institute, Kyoto University*

⁴*JSPS*

INTRODUCTION

The formation of the correct disulfide bonds are the results of thiol/disulfide exchange reactions that occur during protein folding. Such reactions are thermodynamically and kinetically related to the redox potential of the biological system [1]. Thus, *in vitro* folding experiments of proteins containing disulfide bonds are typically carried out in the presence of redox reagents, such as glutathione, cysteine, and protein disulfide isomerase (PDI). We recently reported that a positively charged redox reagent is preferred for accelerating disulfide-exchange reactions, as evidenced by the fact that the folding recovery is greater than that for a typical redox system [2]. Although the formation of disulfide bonds and the tertiary structure of a target protein is affected by a designed redox reagent, the nature of the redox environment its relationship with protein folding remains a matter of debate. Here, we report on the development of a redox reagent for effective folding by means of a new approach.

MATERIALS AND METHODS

Peptide Synthesis-The peptides were synthesized by the Fmoc solid-phase method on using a PSSM-8 peptide synthesizer (Simadzu Corporation, Kyoto) as redox reagents. The resulting peptides, containing two cysteine residues, were air-oxidized to form an intramolecular disulfide bond and the product was purified by RP-HPLC (Hitachi High-Technologies Corporation, Tokyo). The purified peptides were dissolved in 0.1 M Tris/HCl buffer (pH 8.0) and stored at room temperature until used.

Preparation of reduced/denatured lysozyme-The reduced/denatured lysozyme was prepared according to previously method [2], that is, lysozyme was dissolved in 0.1 M Tris/HCl (pH 8.3) containing 20 mM dithiothreitol and 8 M urea, and the solution was allowed to stand for 3 h for room temperature. The reaction mixture was then dialyzed against 10 mM HCl and lyophilized.

Kinetic analyses-The refolding reaction of lysozyme was performed in 0.1 M Tris-HCl (pH 8.0) buffer con-

taining 1.0 mM GSH and 0.2 mM GSSG in the presence or absence of 1 mM synthesized peptide (peptide A or B). A *Micrococcus luteus* suspension (0.5 mg/mL) in 50 mM phosphate buffer (pH 6.5) was prepared to determine the bacteriolysis activity. The bacteriolysis reaction was started by mixing 10 μ L the refolded lysozyme solution and a *Micrococcus luteus* suspension, and was quenched each time by adding a quenching solution containing 0.5 M IAA, 1 M KOH, 1 M Tris/HCl buffer (pH 7.0). The light scattering intensity of the reaction mixtures were measured at 600 nm.

RESULTS

Reduced/denatured lysozyme was employed as a model protein, in order to estimate the folding recovery and velocity of the reaction. The result indicated that the folding recovery in the presence of peptide A or B was greater than that for a typical glutathione redox system. Kinetic analyses revealed that the velocity of folding using a glutathione redox system containing peptide A or B was faster than that using only a glutathione redox system, suggesting that the high recovery is due to its acceleration in the synthesized peptide-assisted folding.

In addition, folding experiments were undertaken using only peptides A or B to evaluate their folding ability. This result showed that only peptide A or B possesses the ability to recover reduced/denatured lysozyme. In general, disulfide-containing proteins such as lysozyme require redox condition to fold correctly *in vivo* or *in vitro*, because proteins in which cysteine residues are involved in folding are folded into the native conformation *via* the formation of complex disulfide intermediates under redox conditions. Thus, GSSG functions as an oxidant in the formation of disulfide bonds in proteins and GSH functions as a reducing agent that cleaves mis-folded disulfide bonds in proteins *in vivo* or *in vitro*, resulting in the formation of a target protein with a thermodynamically stable conformation. Because of this, the synthesized peptide A or B is a redox molecule.

These findings show that a redox molecule is preferred in accelerating the folding reaction and the new method using synthesized peptides is effective in mediating the formation of the native conformation.

REFERENCES

- [1] J.L. Arolas, F.X. Aviles, J.Y. Chang, and S. Ventura. *Trends Biochem Sci* **31** (2006) 292-301.
- [2] M. Okumura, M. Saiki, H. Yamaguchi, and Y. Hidaka. *FEBS Journal* **278** (2011) 1137-1144.

CO6-7 The Preliminary Neutron Experiment for Neutron Biology Using 4CND

T. Chatake, A. Kawaguchi, S. Fujiwara¹, Y. Yanagisawa² and Y. Morimoto.

Research Reactor Institute, Kyoto University

¹Japan Atomic Energy Research Agency

²Chiba Institute of Science

INTRODUCTION: 4CND is the neutron four-circle diffractometer located at B3 port in the neutron reactor of Research Reactor Institute, Kyoto University (KUR) [1]. In the present study, a new application of 4CND was carried out toward contributing neutron biology.

Because of low flux of neutron beam, neutron diffractions from crystals or solutions of macromolecules cannot be collected using 4CND at present. Therefore, in order to apply 4CND to neutron biology, it is necessary to find a new application other than general uses of 4CND. In this study, we applied 4CND to study a chemical reaction of a protein and a carborane compound induced by neutron irradiation.

Crystals of a complex of hen-egg-white lysozyme (HEWL) and a carborane drug (KG2-112), shown in Fig. 1, was prepared for this study. The crystal structure of this complex was examined by X-ray crystallographic analysis to check the quality of the crystal and the isomorphism between HEWLs with and without KG2-112. After the preliminary X-ray analysis, neutron experiment was carried out.

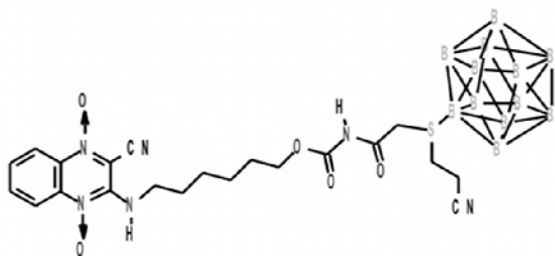


Fig. 1. The chemical structure of the KG2-112.

EXPERIMENTS: Crystallization was carried out using the sitting vapor diffusion technique. 20 μ l of crystallization solution, containing 20 mg/ml HEWL, 0.1 mol/l sodium acetate (pH 4.7) and 0.5 X_{NaCl} mol/l NaCl, was equilibrated by 700 μ l of reservoir solution, containing 0.1 mol/l sodium acetate (pH 4.7), X_{NaCl} mol/l NaCl, where X_{NaCl} is in the range from 0.8 to 1.2. The introduction of KG2-112 was carried out by the co-crystallization technique. The concentration of KG2-112 in the crystallization solution was 1.25 mmol/l. This value is comparative to the concentration of HEWL (1.39 mmol/l).

X-ray experiment was carried out using synchrotron radiation at BL38B1 in Spring-8. The crystals of HEWL with and without KG2-112 (apoHEWL and holoHEWL, respectively) were flash-cooled by N₂ gas, and their X-ray

diffraction data sets were collected at 100K. Structure determinations were carried out by the molecular replacement method, using atomic coordinates of 193L as a probe. Modelings and refinements of their atomic structures were carried out using the programs Phenix [2] and Coot [3].

Neutron experiment was carried out using 4CND. Crystals were sealed with crystallization solution into a glass capillary ($\phi = 1.0$ mm), and then the capillary was mounted on the goniometer of 4CND. 17.5 h exposure at 1MW operation and 2 h exposure at 5MW operation were carried out.

RESULTS: Crystals of holoHEWL and apoHEWL were obtained as shown in Fig. 2. The apoHEWL is colorless like other HEWL crystals reported previously. Meanwhile, holoHEWL is colored in red, because KG2-112 is red in solution. The growths of these crystals were also different. In case of apoHEWL, only crystals appeared in crystallization solution. On the other hand, red precipitation occurred in crystallization solution of holoHEWL immediately after the preparation of crystallization solution, and then red apoHEWL crystals appeared from the precipitation and the precipitation decreased.



Fig. 2. Crystals of the HEWL-KG112 complex (left: $X_{\text{NaCl}} = 0.8$) and only HEWL (right: $X_{\text{NaCl}} = 1.2$).

X-ray analyses showed that the holoHEWL crystal was isomorphous with the apoHEWL crystal. Crystal structures of both of the apo- and holo- HEWL were determined at 1.45 \AA resolution. Electron densities, which would be expected to correspond to KG2-112, were observed in the solvent region of the crystal structure of holoHEWL.

We are planning to carry out X-ray crystallographic analysis of holo- and apo- HEWL crystals, which were exposed by neutron beam at 4CND.

REFERENCES:

- [1] Shibuya *et al.*, Annual Reports of the Research Reactor Institute, Kyoto University (1968) 124-136.
- [2] P. D. Adams *et al.*, Acta Cryst. D66 (2010) 213-221.
- [3] P. Emsley *et al.*, Acta Cryst. D66 (2010) 486-501.